




RESEARCH ARTICLE

Optimized psilocybin production in tryptophan catabolism-repressed fungi

Slavica Janevska¹  | Sophie Weiser^{2,3}  | Ying Huang^{4,5} | Jun Lin⁴ |
 Sandra Hoefgen⁴  | Katarina Jojić⁴ | Amelia E. Barber⁶ | Tim Schäfer^{7,8} |
 Janis Fricke^{7,8} | Dirk Hoffmeister^{7,8} | Lars Regestein² | Vito Valiante⁴ |
 Johann E. Kufs² 

¹(Epi-)Genetic Regulation of Fungal Virulence, Leibniz Institute for Natural Product Research and Infection Biology–Hans Knöll Institute, Jena, Germany

²Bio Pilot Plant, Leibniz Institute for Natural Product Research and Infection Biology–Hans Knöll Institute, Jena, Germany

³Faculty of Biological Sciences, Friedrich Schiller University, Jena, Germany

⁴Biobricks of Microbial Natural Product Syntheses, Leibniz Institute for Natural Product Research and Infection Biology–Hans Knöll Institute, Jena, Germany

⁵Paleobiotechnology, Leibniz Institute for Natural Product Research and Infection Biology–Hans Knöll Institute, Jena, Germany

⁶Fungal Informatics, Friedrich Schiller University, Jena, Germany

⁷Pharmaceutical Microbiology, Friedrich Schiller University, Jena, Germany

⁸Pharmaceutical Microbiology, Leibniz Institute for Natural Product Research and Infection Biology–Hans Knöll Institute, Jena, Germany

Correspondence

Slavica Janevska, (Epi-)Genetic Regulation of Fungal Virulence, Leibniz Institute for Natural Product Research and Infection Biology–Hans Knöll Institute, Jena, Germany.
 Email: slavica.janevska@leibniz-hki.de

Johann E. Kufs, Bio Pilot Plant, Leibniz Institute for Natural Product Research and Infection Biology–Hans Knöll Institute, Jena, Germany.
 Email: johann.kufs@uni-bielefeld.de

Present address

Johann E. Kufs, AG Genome Engineering and Editing, Bielefeld University, Bielefeld, Germany

Funding information

European Social Fund, Grant/Award Number: 2019FGR0079 and 2022FGR0007; Bundesministerium für Bildung und Forschung; Deutsche Forschungsgemeinschaft—SFB 1127, Grant/Award Number: 239748522; Germany's Excellence Strategy—EXC 2051, Grant/Award Number: 390713860

Abstract

The high therapeutic potential of psilocybin, a prodrug of the psychotropic psilocin, holds great promise for the treatment of mental disorders such as therapy-refractory depression, alcohol use disorder and anorexia nervosa. Psilocybin has been designated a 'Breakthrough Therapy' by the US Food and Drug Administration, and therefore a sustainable production process must be established to meet future market demands. Here, we present the development of an in vivo psilocybin production chassis based on repression of L-tryptophan catabolism. We demonstrate the proof of principle in *Saccharomyces cerevisiae* expressing the psilocybin biosynthetic genes. Deletion of the two aminotransferase genes *ARO8/9* and the indoleamine 2,3-dioxygenase gene *BNA2* yielded a fivefold increase of psilocybin titre. We transferred this knowledge to the filamentous fungus *Aspergillus nidulans* and identified functional *ARO8/9* orthologs involved in fungal L-tryptophan catabolism by genome mining and cross-complementation. The double deletion mutant of *A. nidulans* resulted in a 10-fold increased psilocybin production. Process optimization based on respiratory activity measurements led to a final psilocybin titre of 267 mg/L in batch cultures with a space–time–yield of 3.7 mg/L/h. These results demonstrate the suitability of our engineered *A. nidulans* to serve as a production strain for psilocybin and other tryptamine-derived pharmaceuticals.

Slavica Janevska and Sophie Weiser contributed equally to this work.

This is an open access article under the terms of the [Creative Commons Attribution-NonCommercial](https://creativecommons.org/licenses/by-nc/4.0/) License, which permits use, distribution and reproduction in any medium, provided the original work is properly cited and is not used for commercial purposes.

© 2024 The Author(s). *Microbial Biotechnology* published by John Wiley & Sons Ltd.

INTRODUCTION

Psilocybin, a mushroom indolyethylamine alkaloid, represents the chemically stable prodrug of the psychotropic 4-dephosphoryl analog psilocin (Hofmann et al., 1959). The latter is structurally related to serotonin and acts as a partial agonist of the human serotonin receptor 2B (5-HT_{2B}) (Fricke et al., 2019). Numerous recent clinical studies convincingly underscored psilocybin's potential to treat patients suffering from therapy-refractory depression, alcohol use disorder and anorexia nervosa (Goodwin et al., 2022; Jensen et al., 2022; Peck et al., 2023), convincing the US Food and Drug Administration to grant psilocybin with the status of 'Breakthrough Therapy', meaning that this candidate (pro)drug may prove substantially superior to current therapies.

The re-discovered pharmaceutical value of psilocybin has entailed an increased demand for the compound. The molecule has traditionally been produced by total synthesis, for which several protocols have been devised (Fricke et al., 2019). However, the characterization of the biosynthetic enzymes in the 'magic mushroom' *Psilocybe cubensis* set the stage for a biotechnological large-scale psilocybin production (Fricke et al., 2017). The first approach was a cell-free biosynthesis through a three-enzyme in vitro route from the synthetic precursor 4-hydroxy-L-tryptophan to psilocybin. This method harnesses the L-tryptophan decarboxylase PsiD, the kinase PsiK and the methyltransferase PsiM. These three enzymes, together with

the regioselective cytochrome P₄₅₀-monooxygenase PsiH, constitute the complete biosynthetic pathway in *Psilocybe* mushrooms (Blei et al., 2018) (Figure 1A).

A second approach was to produce psilocybin heterologously in chassis organisms. To this aim, the filamentous fungus *Aspergillus nidulans* was previously equipped with a versatile polycistronic expression system for biosynthetic pathways, established for various hosts (Hoefgen et al., 2018; Reimer et al., 2022). Later on, higher titres of 1.16 g/L psilocybin were obtained by fermenting *Escherichia coli* expressing *psiK*, *psiM* and *psiD*. However, in this case, a targeted feeding with 4-hydroxyindole was necessary to compensate for the missing P₄₅₀-monooxygenase PsiH (Adams et al., 2019). De novo psilocybin synthesis was established in bacteria by producing PsiH and a cytochrome P₄₅₀ reductase partner in a separate *E. coli* strain and co-cultivation of both strains yielded 28.5 mg/L psilocybin (Flower et al., 2023). Finally, a successful high-scale production of psilocybin in *Saccharomyces cerevisiae* was obtained by enhancing the native tryptophan biosynthesis and implementing the availability of tryptamine (Milne et al., 2020). However, this approach does not take catabolic routes into account that potentially compete for L-tryptophan.

Breakdown of tryptophan has been well characterized in *S. cerevisiae* (Figure 1B) and is mainly initiated by the heme-dependent indoleamine 2,3-dioxygenase Bna2 (Yuasa & Ball, 2011). It oxidatively converts L-tryptophan to *N*-formyl-L-kynurenine, which is then modified to L-kynurenine by the kynurenine

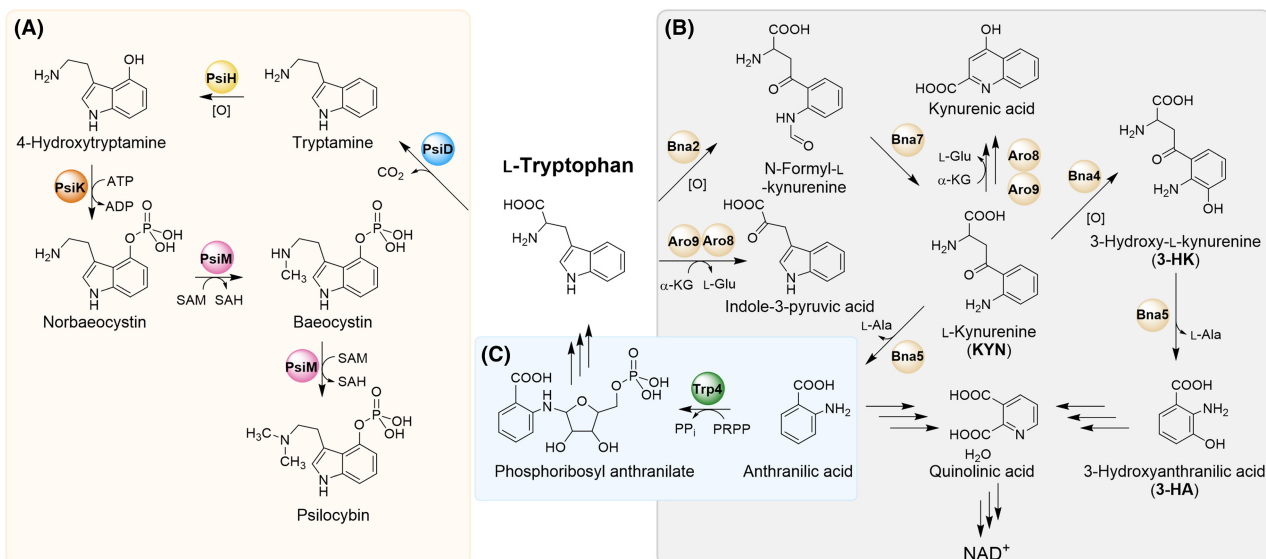


FIGURE 1 Schematic, simplified overview on L-tryptophan metabolism. (A) Four-enzyme psilocybin biosynthetic pathway, reconstituted in *S. cerevisiae*. (B) In *S. cerevisiae*, L-tryptophan is deaminated to indole-3-pyruvic acid by the aminotransferases Aro8 and Aro9. A second catabolic route includes oxidative cleavage of the pyrrole ring of L-tryptophan by the indoleamine-2,3-dioxygenase Bna2, to yield *N*-formyl-L-kynurenine, that is a precursor for the biosynthesis of both kynurenic acid and quinolinic acid. The latter is required for nicotinamide adenine dinucleotide biosynthesis. (C) De novo biosynthesis of L-tryptophan via the anthranilate phosphoribosyltransferase Trp4. L-Ala, L-alanine; L-Glu, L-glutamate; NAD⁺, nicotinamide adenine dinucleotide; PRPP, 5-phospho- α -D-ribose-1-diphosphate; SAH, S-adenosyl-L-homocysteine; SAM, S-adenosyl-L-methionine; α -KG, α -ketoglutaric acid.

formamidase Bna7 (Wogulis et al., 2008). A further relevant step, performed by the kynureninase Bna5, is then the cleavage of L-kynurenine to form L-alanine and anthranilic acid (Panozzo et al., 2002). Bna5 can also cleave 3-hydroxy-L-kynurenine, releasing 3-hydroxyanthranilic acid (Kim et al., 2018). Subsequently, the two acids produced are precursors in the biosynthesis of quinolinic acid, which after decarboxylation to nicotinic acid serves NAD⁺ biosynthesis, but also as precursors in the de novo biosynthesis of L-tryptophan via the anthranilate phosphoribosyltransferase Trp4 (Furter et al., 1986) (Figure 1C). The catabolism of tryptophan can also occur via amino acid transamination by Aro8 and Aro9, the two α -ketoglutarate-dependent aminotransferases present in *S. cerevisiae* (Iraqui et al., 1998).

Several indoleamine 2,3-dioxygenases have already been characterized in filamentous fungi. In particular, filamentous ascomycetes harbour three BNA2-like genes, named *idoA*, *idoB* and *idoC* (Yuasa & Ball, 2011). Deletion of *idoA* has major effects on virulence in both the plant pathogenic fungus *Fusarium graminearum* and the opportunistic human pathogen *Aspergillus fumigatus* (Liu et al., 2023; Zelante et al., 2021). Moreover, the *aroH* gene product has been biochemically characterized in *A. fumigatus*, confirming its role as a pyridoxal 5'-phosphate (PLP)-dependent aminotransferase involved in tryptophan transamination (Dindo et al., 2018).

In addition to the two major pathways, fungi can use L-tryptophan as a scaffold to produce indole acetate or secondary metabolites. One example is the aforementioned conversion of tryptophan to tryptamine by tryptophan decarboxylases, as reported in *P. cubensis* and *Rhizoctonia solani* (Fricke et al., 2017; Pedras et al., 2005). A combined genetic, biochemical and transcriptomic study within the psilocybin producer *Psilocybe mexicana* showed a massive downregulation of L-tryptophan catabolism genes, among them *iasA*, encoding an indole-3-acetaldehyde synthase, when psilocybin biosynthesis set in (Seibold et al., 2024). Additionally, fungi may produce secondary metabolite-specific enzymes with catalytic similarities to those of primary metabolism, such as the aminotransferase TdiD, which is part of the gene cluster that mediates the biosynthesis of terrequinone A in *A. nidulans* (Bouhired et al., 2007; Schneider et al., 2007), or the indoleamine 2,3-dioxygenases involved in the biosynthesis of benzazepine alkaloids (Caesar et al., 2020; Chen et al., 2022; Li et al., 2020).

Here, we report on a strategy to obtain high psilocybin titres in fungal heterologous hosts by suppressing L-tryptophan catabolism and increasing its intracellular availability. For a proof of concept, we expressed the psilocybin biosynthetic gene cluster (BGC) in an *S. cerevisiae* triple mutant deficient in genes encoding L-tryptophan-degrading enzymes, namely ARO8,

ARO9 and BNA2. Batch cultures yielded approximately 50 mg/L of psilocybin. To reach the highest production titres possible, we implemented the concept of suppressing L-tryptophan catabolism in the mould *A. nidulans* as well. We successfully identified and deleted two genes coding for functional Aro8/Aro9 orthologs. This approach yielded a strain capable of producing 267 mg/L psilocybin in batch cultures. The herein generated production strain will enable the development of a sustainable, reproducible and scalable biotechnological production process for the pharmaceutically relevant prodrug psilocybin.

EXPERIMENTAL PROCEDURE

Strains, media and growth conditions

The wild-type strain *S. cerevisiae* BY4741, Δ *aro8* and Δ *aro9* single mutant derivatives and Δ *bna2* were retrieved from Euroscarf (Scientific Research and Development GmbH, Oberursel, Germany). In preparation for yeast transformation, strains were grown in YPD complete medium. Selection and cultivation of transformants were performed using SD minimal media with the appropriate dropout amino acid solution. For the production of psilocybin, L-kynurenine and anthranilic acid, an SD -Uracil/Uridine (-Ura) pre-culture was prepared overnight. The main culture consisted of 20 mL SD -Ura +1 mM L-tryptophan in 100 mL triple-baffled Erlenmeyer flasks and was inoculated with the pre-culture to give an OD₆₀₀ of 0.5. All strains were grown in triplicates at 30°C and 180 rpm for 2 days. For plate assays, the SD -Ura overnight culture was diluted with water to OD₆₀₀ = 0.1–1 × 10⁻⁴ and 10 μ L of each dilution was incubated on selective plates (SD -Ura +/- Trp) for 3 days.

The cultivations of *A. nidulans* were performed in *Aspergillus* minimal medium (AMM) consisting of 6 g/L NaNO₃, 0.52 g/L KCl, 1.52 g/L KH₂PO₄, 0.52 g/L MgSO₄ × 7 H₂O and 1 mL/L Hutner's trace elements. The Hutner's trace elements were prepared as 1000× stock solution and contained 50 g/L EDTA, 22 g/L ZnSO₄ × 7 H₂O, 11 g/L H₃BO₃, 5 g/L MnCl₂ × 4 H₂O, 1.6 g/L CoCl₂ × 6 H₂O, 1.6 g/L CuSO₄ × 5 H₂O, 1.1 g/L (NH₄)₆Mo₇O₂₄ × 4 H₂O and 5 g/L FeSO₄ × 7 H₂O. For expression analysis of the *A. nidulans* wild-type strain RMSO11, 50 mL AMM (supplemented with 3 mg/L *p*-aminobenzoic acid and 5 mM L-arginine) was inoculated with 1 × 10⁷ conidia/mL in a 300 mL Erlenmeyer flask and shaken for 1 day at 37°C and 180 rpm. To induce gene expression, the mycelium was shifted to new flasks with or without 10 mM L-tryptophan for 1 h. Expression analysis via qRT-PCR was performed as previously described (Janevska et al., 2020) with primers listed in Table S2. For *A. nidulans* plate assays, AMM (with *p*-aminobenzoic acid and L-arginine) was

supplemented with 5/10 mM L-tryptophan or 5 mM nicotinamide and serial 1:10 spore dilutions started with a 5 μ L drop of 1×10^5 conidia/mL. Single drops in the centre of the plate were 5 μ L of 1×10^3 conidia/mL.

For psilocybin production in *A. nidulans*, 1×10^7 conidia/mL were inoculated in 50 mL AMM in a 300 mL Erlenmeyer flask with supplementation of 3 mg/L *p*-aminobenzoic acid, 5 mM L-arginine, 1 mM L-tryptophan, 0.1 mM nicotinamide and 10% (w/v) glucose, cultivated for 18 h in shaking condition at 37°C, 180 rpm. Afterwards, 20 μ g/mL doxycycline was added to induce the expression of the *psi* gene cluster. Then, incubation continued for another 24 h at 37°C and 180 rpm.

Plasmid construction and generation of transformants

To construct the yeast *psi* expression plasmid pYes-*psi*, the previously created promoterless plasmid pJF33 harbouring all psilocybin biosynthetic genes in the order *psiH*, *psiD*, *psiK* and *psiM* and the *tev* protease-coding sequence was used (Hoefgen et al., 2018). A PCR fragment obtained from the empty overexpression plasmid pYes2-*TEF1* (Hoefgen et al., 2018), amplified with primers [1]//[2] (Table S2), was used together with the *PacI*-treated pJF33 to obtain pJF34 based on transformation-associated recombination (TAR) cloning using the protocol reported by Hoefgen et al. (2018). Then, *venusN* and *venusC* were removed by amplification based on pJF34 with primer pairs [3]//[4] and [5]//[6]. These two fragments were assembled by TAR cloning to give pYes-*psi*. This plasmid harbours the psilocybin polycistronic cluster under the control of the *TEF1* promoter, 2 μ as origin of replication and *URA3* as auxotrophic marker and was subsequently used to transform *S. cerevisiae* strains.

The generation of yeast double and triple mutants was achieved by homologous recombination. *ARO8* was exchanged for *LEU2* in the Δ *aro9* background using flanks of ca. 500 bp. The *ARO8* deletion construct was generated by fusion PCR. Therefore, *ARO8* upstream and downstream flanks including the required overhangs were amplified with oligonucleotide primer pairs [7]//[8] and [11]//[12] (Table S2), respectively, using genomic DNA of *S. cerevisiae* BY4741 as template. *LEU2* including overhangs was amplified with primer pair [9]//[10], using genomic DNA of a prototrophic yeast as template (Jena Microbial Research Collection, JMRC: STI25222). The fusion PCR was performed by applying the three PCR products and the outer primers [7]//[12].

Furthermore, *S. cerevisiae* *BNA2* was exchanged for *HIS3* in the Δ *aro8*/ Δ *aro9* background. The *BNA2* deletion construct was generated by TAR cloning. Therefore, *BNA2* upstream and downstream flanks of ca. 900 bp

including the required overhangs were amplified with primer pairs [13]//[14] and [15]//[16] (Table S2), respectively, based on genomic DNA of *S. cerevisiae* BY4741. *HIS3* including promoter and terminator sequences was amplified with the primer pair [17]//[18], based on genomic DNA of the prototrophic yeast STI25222. *S. cerevisiae* BY4741 was transformed with the three PCR products as well as with the *HindIII*/*XbaI*-digested shuttle vector pYes2 (Life Technologies, Darmstadt, Germany), to create the deletion vector p Δ *bna2*. For the transformation of Δ *aro8*/ Δ *aro9*, the *BNA2* deletion construct was amplified with primers [13]//[16] from the deletion vector and the PCR reaction was *DpnI*-digested to remove the template.

For complementation of *S. cerevisiae* Δ *aro8*/ Δ *aro9*, *A. nidulans* potential *aro*-like aminotransferase genes were amplified from cDNA: *aroH1* [19]//[20], *aroH2* [21]//[22], *aroI1* [23]//[24], *aroI2* [25]//[26], *tdiD* [27]//[28] and *ANIA_00780* [29]//[30] (Table S2). As controls, *S. cerevisiae* *ARO8* [31]//[32] and *ARO9* [33]//[34] were amplified from gDNA of BY4741. The inserts were cloned into *HindIII*/*BamHI*-digested pYes2-*TEF1* via primer-introduced overhangs and TAR cloning.

Similarly, to complement *S. cerevisiae* Δ *bna2*, *A. nidulans* potential *ido*-like indoleamine 2,3-dioxygenase genes were amplified from cDNA: *idoA* [35]//[36], *idoB* [37]//[38] and *idoC* [39]//[40] (Table S2). For complementation of *S. cerevisiae* Δ *bna5*, *A. nidulans* *kynU2* [41]//[42] was amplified. As controls, *S. cerevisiae* *BNA2* [43]//[44] and *BNA5* [45]//[46] were amplified from gDNA of BY4741.

To delete *A. nidulans* *aroH1*, ca. 1 kb flanks were amplified with primers [47]//[48] and [49]//[50] using gDNA of *A. nidulans* RMSO11 wild type (Table S2). The *pabA* resistance gene (An03g03130), including its promoter and terminator, was amplified with [51]//[52] from *Aspergillus niger* gDNA. The fusion PCR was performed by applying the three PCR products and the outer primers [47]//[50]. Similarly, to delete *A. nidulans* *aroH2*, ca. 1 kb flanks were amplified with [53]//[54] and [55]//[56] from RMSO11 gDNA. The *ptrA* resistance cassette was amplified with primers [57]//[58] and plasmid pSK275 as template (Krappmann et al., 2006). Then, the fusion PCR was performed with the outer primers [53]//[56]. Finally, to delete *A. nidulans* *idoA*, ca. 1 kb flanks were amplified with primers [59]//[60] and [61]//[62] from *A. nidulans* gDNA. The *ptrA* cassette and the fusion PCR [59]//[62] were amplified as described above.

Phylogenetic analysis

RefSeq Fungi Database files were downloaded from the National Center for Biotechnology Information (NCBI). The search for conserved amino acids in fungal genomes was carried out using the BLAST® Command

Line Applications (Camacho et al., 2009). The search was performed using standard default parameters. Hits were extracted and double-checked using the CDD Database.

Amino acid sequences for the ARO- and IDO-like proteins (Table S1) were aligned using MUSCLE (Edgar, 2004) v3.8 with a maximum of 16 iterations. Phylogenetic inference was performed using IQ-TREE2 (Minh et al., 2020) v2.2.0.3 and 1000 ultra-fast bootstraps. The ModelFinder (Kalyaanamoorthy et al., 2017) module of IQ-TREE2 was used to identify JTT+I+G4 (Jones et al., 1992) as the best-fitting substitution model for both ortholog sets. Phylogenetic trees were visualized using ggtree (Yu et al., 2017).

Chemical analysis

After the cultivation of yeast, 300 μ L of the culture was mixed with 300 μ L MeOH prior to bead milling. Then, samples were filtered for LC-HRMS analysis (samples were 1:2 dilutions).

After the cultivation of *A. nidulans*, 20 mL culture together with 10 mL H₂O and 10 mL MeOH was homogenized. Then, 100 μ L of crude extract was pipetted with a cut tip and diluted with 900 μ L H₂O, filtered and analysed by LC-HRMS (samples were diluted 1:20).

LC-HRMS was performed on a Q-Exactive Plus Hybrid Quadrupole Orbitrap mass spectrometer using electrospray ionization and a Dionex UltiMate 3000 UHPLC system (Thermo Fisher Scientific) equipped with a Kinetex C₁₈ column (2.1 \times 150 mm, 2.5 μ m, 100 Å , Phenomenex). The analytical method is a gradient elution of solvents A (water, 0.1%, v/v, formic acid) and B (acetonitrile, 0.1%, v/v, formic acid) at a flow rate of 0.3 mL/min: 5% B for 0.5 min, a linear gradient to 97% B for 11.5 min, then 97% B for 3 min and 5% B for 3 min. Calibration curves for psilocybin, baeocystin and psilocin were determined using peak areas of HPLC-HRMS measurements of samples with concentration ranges from 0 to 10, 0 to 68 and 0 to 0.625 μ M, respectively. All samples were analysed in triplicates and error bars represent the standard error.

HPLC method organic acids

Organic acids and ethanol were analysed by HPLC. The X-LC® system (JASCO International Co., Tokyo, Japan) was equipped with an Aminex HPX-87H Ion Exclusion Column (300 \times 7.8 mm, 9 μ m, Bio-Rad Laboratories Inc., Hercules CA, USA), maintained at 50 °C, a refractive index detector and an UV detector (210 nm). The substances were separated under isocratic conditions with 0.5 mL/min of 0.005 M H₂SO₄ as the mobile phase. For injection, 50 μ L of diluted culture filtrate (1:10 with 0.005 M H₂SO₄) was used.

Growth and metabolic activity monitoring

Cultivations were conducted in 250 mL unbaffled shake flasks filled with 30 mL AMM containing 100 g/L glucose, buffered to pH 7.0 with 100 mM 3-(*N*-morpholino) propanesulfonic acid (MOPS) and supplemented with 3 mg/L *p*-aminobenzoic acid, 0.1 mM nicotinamide and 1 mM L-tryptophan. *A. nidulans* strains tJF03 (Hoefgen et al., 2018) and Δ *aroH1*/ Δ *aroH2*_psi were inoculated to 1×10^7 conidia/mL and grown at 300 rpm with 50 mm shaker throw for 192 h. To determine the OTR and CTR, the incubators were equipped with the Kühner Transfer-Rate Online Measurement (TOM) system, enabling online exhaust gas analysis. Aeration with compressed air was set to 11 mL/min and one measuring cycle of 20 min included 6 min measuring time. Psilocybin formation was induced with 50 μ g/mL doxycycline at 31 h after the OTR peaked. For better production of biosynthetic enzymes, the incubation temperature was reduced from 37 to 30 °C. For offline analysis during cultivation, duplicate samples were taken in the form of entire shake flask cultures that were run in parallel.

Offline analytics

To determine the cell dry weight, 10 mL culture broth was vacuum filtrated through a pre-dried and pre-weighed Whatman® 589/2 filter, washed with 100 mL Milli-Q® water and dried and weighed using an MA160 moisture analyser. Glucose concentration was measured in the supernatant using a YSI 2950 Biochemistry Analyser. The pH measurement was conducted with a Schott pH meter. For psilocybin, psilocin and baeocystin extraction, 0.5 mL culture broth was diluted 1:2 with Milli-Q® water. Subsequently, 0.5 mL diluted culture broth was diluted 1:2 with methanol, added to 0.5 g glass beads (0.75–1.0 mm) and milled three times for 60 s at 6.5 m/s and 4 °C (FastPrep -24™ Sample Preparation System) for cell disruption. The cell lysate was centrifuged at 17,000 g, 4 °C for 10 min and the supernatant was diluted 1:5 with Milli-Q® water before filtering through 0.22 μ m cellulose acetate syringe filters and storing at -20 °C until analysis. For each sample, triplicate extraction was performed.

RESULTS AND DISCUSSION

Psilocybin production in L-tryptophan catabolism-repressed *S. cerevisiae*

The removal of competing pathways is one of the most commonly used strategies in metabolic engineering to enhance precursor supply (Lee et al., 2012; Qian et al., 2011). Therefore, we hypothesized that disabling L-tryptophan degradation in the production host

would route the available cellular L-tryptophan pool preferentially towards psilocybin biosynthesis. To test this hypothesis, the *psi* cluster was expressed in *S. cerevisiae* strains deficient for either the *ARO8*, the *ARO9* (aminotransferases) or *BNA2* (indoleamine 2,3-dioxygenase) genes. Deletion of *ARO9* resulted in mutants that were more sensitive to elevated L-tryptophan concentrations (5mM). The concomitant deletion of *ARO8* in the Δ *aro9* background increased this sensitivity, which rendered double mutants unable to grow in the presence of 5mM L-tryptophan and confirmed previous results (Figure 2A) (Ohashi et al., 2017). However, the additional deletion of *BNA2*, resulting in the triple mutant Δ 3, did not show increased sensitivity towards L-tryptophan in comparison to the double mutant, indicating that the production of kynurenic acid does not contribute to the detoxification

of excess L-tryptophan (Figure 2A). Based on these results, *S. cerevisiae* production cultures contained 1mM L-tryptophan, which allowed for robust growth of all strains.

The plasmid harbouring the psilocybin biosynthetic genes (Figure 2B) was used to transform the Δ *aro8*, Δ *aro9*, and Δ *bna2* single mutants, the Δ *aro8*/ Δ *aro9* double mutant and a mutant lacking all three genes (Δ 3). Quantitative analysis revealed that psilocybin production had increased in the single mutants, compared to the wild-type control expressing the *psi* cluster (Figure 2C). In particular, the production of baecocystin, that is, the monomethylated immediate precursor to psilocybin, was significantly higher in the Δ *aro9* mutant strain, suggesting a more active pathway as consequence of disabled L-tryptophan catabolism. For full conversion of baecocystin to psilocybin, additional copies of the *psiM* methyltransferase gene could be integrated into the *psi* cluster as previously shown (Milne et al., 2020).

The above results suggested that the more severely L-tryptophan catabolism is blocked, the better the heterologous psilocybin pathway would function as the sole sink for this amino acid (Lee et al., 2012; Qian et al., 2011). To test this hypothesis and strongly inhibit L-tryptophan catabolism, the Δ *aro8*/ Δ *aro9* double mutant and Δ 3 triple mutant with the plasmid harbouring the *psi* cluster were analysed (Figure 2C). For the Δ *aro8*/ Δ *aro9* double mutant background, we observed a significantly increased psilocybin production while the baecocystin level was similar to that of the single Δ *aro9* background. This trend was also observed for the Δ 3 mutant background, where psilocybin titres were further increased to 34.3mg/L, but not baecocystin titres. Curiously, the latter mutants, which produced higher titres of psilocybin and baecocystin, showed strongly reduced levels of psilocin, pointing towards more stable production of psilocybin and reduced dephosphorylation compared to Milne et al. (2020). Overall, the expression of the polycistronic *psi* cluster yielded ~7.5 mg/L of psilocybin and ~5 mg/L of baecocystin in the wild-type background while the repression of the genes involved in L-tryptophan catabolism led to up to fivefold higher psilocybin titres. Nevertheless, these titres were still fivefold lower than those produced by a strain from Milne et al. (2020). The reason for that is likely the lack of an appropriate cytochrome P_{450} reductase responsible for the transfer of electrons between NADPH and the cytochrome P_{450} enzyme PsiH.

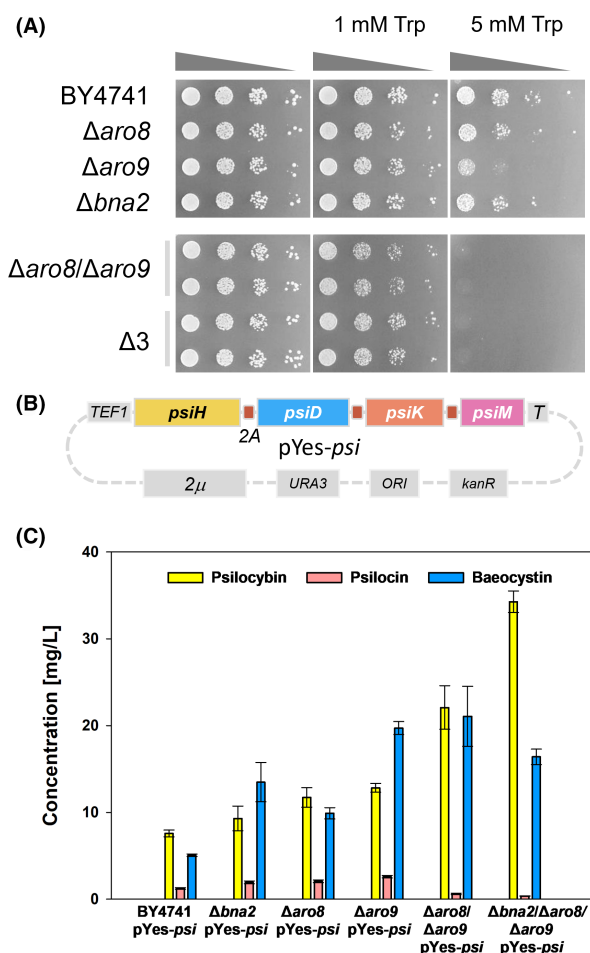


FIGURE 2 Psilocybin production in *S. cerevisiae* mutant strains. (A) The phenotypic analysis of L-tryptophan catabolism-repressed *S. cerevisiae* confirmed their sensitivity to high L-tryptophan (Trp) concentrations. (B) Genetic map of the expression plasmid pYes-*psi* carrying the *psi* cluster expressed as a polycistron under the control of the constitutive *TEF1* promoter. (C) Production of psilocybin, psilocin and baecocystin in *S. cerevisiae* wild type and tryptophan catabolism-repressed mutants after 48 h of cultivation.

Tryptophan catabolism in *A. nidulans*

The results obtained in *S. cerevisiae* batch cultures clearly showed the potential of repression of L-tryptophan catabolism to implement psilocybin production. Furthermore, the product spectrum was less diverse and much more

focused on the actual pharmaceutically relevant compound psilocybin, compared to a previous yeast-based approach (Milne et al., 2020). However, the performance of the obtained strains did not seem to quantitatively advance this prior endeavour. We therefore decided to transfer this knowledge to filamentous fungi and study the genes linked to tryptophan catabolism in *Aspergillus*. We chose the model fungus *A. nidulans*, which was also the first chassis used for the heterologous production of psilocybin (Hoefgen et al., 2018).

BLASTp analysis revealed that the *A. nidulans* genome encodes six homologues of potential ARO-like aminotransferases (Table 1). Among them, only the *tdiD* gene has been previously identified as part of the terrequinone A gene cluster (Bok et al., 2006; Schneider et al., 2007). Using the six ARO-like proteins from *A. nidulans* as queries, we performed a BLASTp search on the NCBI RefSeq database (Sayers et al., 2021) and identified highly similar proteins in all represented *Aspergilli* (Table S1). Analysis of the selected sequences using the Conserved Domains Database (CDD) (Wang et al., 2023) confirmed that all of these are putative PLP-dependent aminotransferases and that, in general, each *Aspergillus* genome encodes between four and six ARO-like proteins (Table S1).

Phylogenetic analysis revealed the presence of six clades (Figure 3A). We identified two groups of proteins similar to AroH from *A. fumigatus* (Spizzichino et al., 2022). However, within these clades, we observed a few *Aspergilli* with two AroH-like enzymes, including *A. nidulans*. A second, less represented clade included putative aminotransferases/transaminases similar to AroI from *A. fumigatus* (Choera et al., 2017). Next, the least represented clade (Figure 3A, yellow) refers to proteins similar to TdiD, which were only identified in species containing the respective *tdi* BGC (Figure S1). Finally, a further group included putative and yet uncharacterized transaminases similar to Aro8 from yeast.

To better understand the role of these genes during tryptophan catabolism, we investigated their expression

upon induction by L-tryptophan (Figure 3B). qRT-PCR analysis revealed that *aroH1* and *aroI1* were the only genes with measurable basal expression, which further increased in the presence of higher L-tryptophan concentrations. Next, each corresponding cDNA was cloned into a yeast expression vector and transferred into the *S. cerevisiae* $\Delta aro8/\Delta aro9$ mutant background (Figure 3C). The over-expression of *aroH1* and *aroH2* completely restored the tryptophan sensitivity of the yeast strain, confirming their function as transaminases responsible for indole pyruvic acid production. Moreover, the assay also confirmed the function of TdiD as transaminase, however, the gene is specific to the biosynthesis of terrequinone A and not expressed under laboratory conditions (Figure 3B). Therefore, it was excluded as target for our repression strategy of general tryptophan catabolism. The other expressed genes *aroI1*, *aroI2* and *ANIA_00780* did not complement *S. cerevisiae* $\Delta aro8/\Delta aro9$, suggesting an alternative role for the encoded enzymes.

A second step in the analysis was the search for indoleamine 2,3-dioxygenases (IDOs) that are functionally similar to yeast Bna2. We identified numerous *ido*-like genes in *Aspergilli*. Overall, each *Aspergillus* species harbours three genes encoding potential IDO-like proteins and, as expected, this number may be variable in case of enzymes involved in secondary metabolism (Table 1, Table S1). This situation resembles previous observations for *F. graminearum* and *A. fumigatus* (Liu et al., 2023; Zelante et al., 2021). The phylogenetic analysis resulted in a more scattered tree but, on closer inspection, we could group the potential orthologs not only based on their amino acid sequences but also on gene synteny (Figure 4A). We noticed that *idoB* is encoded adjacent to a putative kynureninase gene, annotated as *kynU2*, which is also potentially involved in tryptophan catabolism (Figure 4B). The two genes share a bidirectional promoter and this locus is present in all *Aspergilli* from the RefSeq Database. Additionally, we noticed this two-gene cluster is commonly present

TABLE 1 BLAST analysis of *A. nidulans* genome for *aro*-like, *ido*-like and kynureninase genes.

Acc. number	Gene name	Function of gene product
ANIA_00780	<i>ANIA_00780</i>	Putative aminotransferase
ANIA_01857	<i>kynU2</i>	Kynureninase
ANIA_01858	<i>idoB</i>	Indoleamine 2,3-dioxygenase
ANIA_02509	<i>idoA</i>	Indoleamine 2,3-dioxygenase
ANIA_09108	<i>idoC</i>	Indoleamine 2,3-dioxygenase
ANIA_04156	<i>aroI2</i>	Putative aminotransferase
ANIA_05041	<i>aroH2</i>	α -Ketoglutarate-dependent aminotransferase
ANIA_06338	<i>aroH1</i>	α -Ketoglutarate-dependent aminotransferase
ANIA_08172	<i>aroI1</i>	Putative aminotransferase
ANIA_08516	<i>tdiD</i>	α -Ketoglutarate-dependent aminotransferase

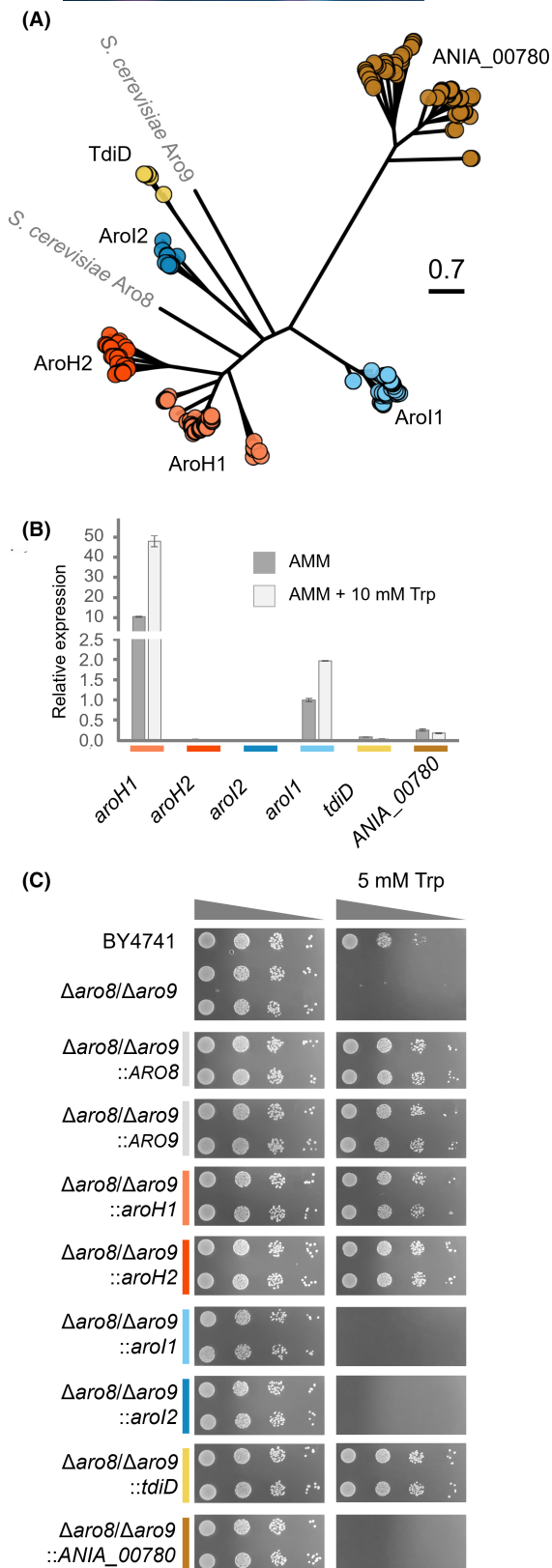


FIGURE 3 Identification and analysis of ARO-like aminotransferases from *A. nidulans*. (A) Evolutionary distance among ARO-like aminotransferases in Aspergilli. Clades are named based on the genes identified in *A. fumigatus* (AroH, AroI) and *A. nidulans* (TdiD). (B) qRT-PCR analysis of the *A. nidulans* aro-like genes in response to tryptophan (Trp). (C) Functional complementation analysis of the identified genes from *A. nidulans* in the *S. cerevisiae* Δ aro8/ Δ aro9 mutant strain. BY4741 and Δ aro8/ Δ aro9 contained the empty plasmid pYes2-TEF1.

A second prominent clade was the one including all IdoA-related enzymes (Figure 4A). In this case as well, we noticed that, in Aspergilli, this gene is generally adjacent to a gene encoding a putative cysteine desulfurase, similar to yeast Nfs1, which catalyses the removal of sulphur from cysteine to gain alanine (Figure 4B) (Kispal et al., 1999). However, this synteny does not seem to be as conserved as that of *idoB* and was mainly found in *Aspergillus* species. Lastly, a third putative indoleamine 2,3-dioxygenase, IdoC, was shown to be highly conserved in Aspergilli, being part of a third large clade in the analysis (Figure 4A).

By performing the phylogenetic analysis, we found that some Aspergilli may contain additional *ido*-like genes, whose functions are difficult to predict. Some of them (Figure 4A, in grey) may be the result of gene duplication. Nonetheless, we observed the formation of clades (Figure 4A, in sky blue), comprising a number of putative indoleamine 2,3-dioxygenases most likely connected to secondary metabolism. All of the genes coding for these enzymes are located in close proximity to natural product genes, for example, AcdA from *Aspergillus candidus*, for the alkaloid pyrrolobenzazepine aspcandine (Chen et al., 2022) and TzpB, related to the biosynthesis of terreazepine (Caesar et al., 2020).

In order to confirm the link between the *ido* genes and tryptophan catabolism, we investigated their gene expression in response to 10 mM L-tryptophan (Figure 4C). While *idoA* expression was not affected by the presence of tryptophan, expression levels of *idoB* and *idoC* were strongly increased. Moreover, the *kynU2* gene was also induced by tryptophan, confirming that the shared promoter regulates both genes. The obtained results confirmed previous observations for *A. fumigatus* (Zelante et al., 2021). The function of the identified genes was further confirmed by complementation of the *S. cerevisiae* loss of function mutants (Figure 4D). As reported, the deletion of *BNA2* blocks the production of L-kynurenine derivatives (via blocking *N*-formyl-L-kynurenine production), while by removing *BNA5* (kynureninase), only the biosynthesis of anthranilic acid is abolished (Figure 1) (Panozzo et al., 2002). We analysed the *S. cerevisiae* Δ bn2 mutant and confirmed that L-kynurenine (KYN), 3-hydroxy-L-kynurenine (3-HK) and 3-hydroxyanthranilic acid (3-HA) were not produced (Figure 4D). In the Δ bn2 mutant strain, we noticed a small peak with the retention time of KYN,

in other filamentous fungi of the Ascomycete division as well, including the *Alternaria*, *Botrytis*, *Fusarium*, *Penicillium*, *Sclerotinia*, *Sordaria* and *Trichoderma* genera, just to mention the most studied ones.

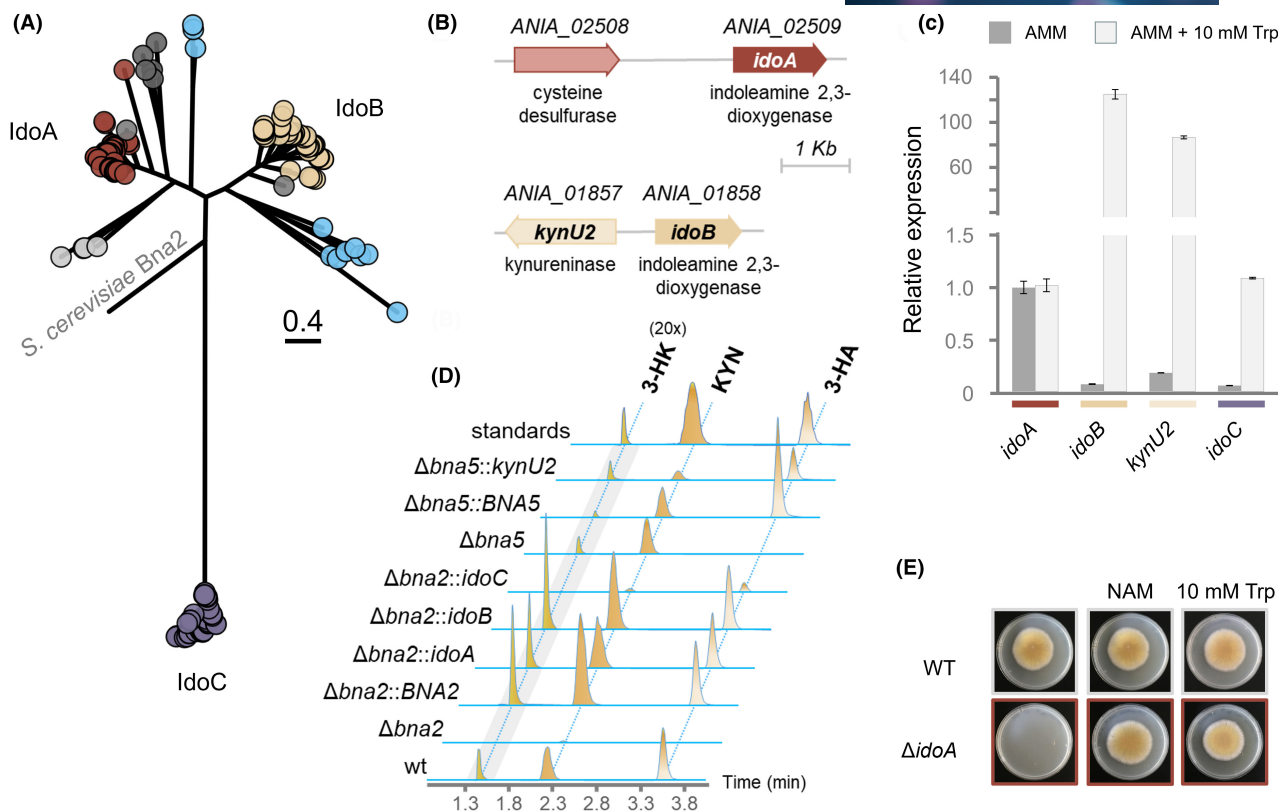


FIGURE 4 Identification and analysis of indoleamine 2,3-dioxygenases from *A. nidulans*. (A) Phylogenetic tree of IDO-like proteins identified in Aspergilli. The three main clades are named based on previous analyses made in *A. fumigatus*. Reported IdoA- and IdoB-related proteins are shown in maroon and sand, respectively, which also show a conserved gene synteny (shown in panel B). IdoC-like proteins are shown in violet, while proteins shown in light blue likely participate in secondary metabolism. The remaining IDO-like proteins are depicted in grey. Scale bar indicates amino acid substitutions/site. (B) Genetic loci for the *idoA* and *idoB* genes in *A. nidulans*. (C) qRT-PCR analysis of the *A. nidulans* *idoA*, *idoB*, *kynU2* and *idoC* genes in response to tryptophan (Trp). (D) Functional complementation of *S. cerevisiae* $\Delta bna5$ mutant and $\Delta bna5$ with *idoA*, *idoB*, *idoC* and *kynU2*, respectively. Corresponding masses are: 3-HK [+m/z] 225.0870; KYN [+m/z] 209.0921; 3-HA [+m/z] 138.0550. (E) Phenotypic analysis of *A. nidulans* $\Delta idoA$ on minimal media and in presence of nicotinamide (NAM) and tryptophan (Trp).

but with a different mass. Functional complementation analysis performed by the expression of *A. nidulans* *idoA*, *idoB* and *idoC* cDNA in the *S. cerevisiae* $\Delta bna2$ background restored the L-tryptophan catabolic pathway. Similarly, the cDNA of *A. nidulans* *kynU2* was able to rescue the loss of 3-HA production in the *S. cerevisiae* $\Delta bna5$ mutant (Figure 4D).

As final proof for the functional conservation of IDO-like proteins in Aspergilli, the deletion of *A. nidulans* *idoA* resulted in a lethal phenotype, when grown on minimal media, which could be rescued by the addition of either nicotinamide or tryptophan (Figure 4E). The latter compound most likely rescues the lethal phenotype by activating the repressed and functionally redundant genes *idoB* and *idoC*.

Psilocybin production in tryptophan catabolism-repressed *A. nidulans*

Analysis of the *A. nidulans* genes potentially involved in tryptophan catabolism suggested the presence of

two main catabolic branches formed by the AroH-like and Ido-like enzymes, respectively. As for the *tdi* BGC, its role in intracellular tryptophan consumption does not seem to be relevant, as *tdiD* was not expressed (Figure 3B) and terrequinone A was not produced under the conditions tested. Complete depletion of *idoA*, *idoB* and *idoC* gene expression has already been shown for *F. graminearum* and *A. fumigatus*, resulting in mutants able to grow only in the presence of nicotinamide, similar to what we are reporting for *A. nidulans* *idoA* deletion here (Figure 4E). For this reason, we focused on the two *aroH* genes characterized here. Growth of the single ($\Delta aroH1$, $\Delta aroH2$) and double mutants ($\Delta aroH1/\Delta aroH2$) was not affected by the addition of up to 10 mM L-tryptophan (Figure S2), suggesting that the *A. nidulans* mutants were more resistant than the respective *S. cerevisiae* mutants (Figure 2A).

The *psi* biosynthetic cluster was expressed as a polycistron without codon optimization under the control of the Tet^{ON} inducible promoter and the analysis of the resulting mutant strains was performed using fluorescent microscopy, exploiting the previously reported

split green fluorescent protein (GFP) system (Hoefgen et al., 2018). Briefly, the psilocybin biosynthetic genes are flanked by two GFP gene subunits and a functional GFP is produced only when the entire mRNA is correctly translated. Consequently, transformants that display a nuclear localization of the GFP correctly express all genes of interest.

The generated single and double deletion mutants of *aroH1* and *aroH2* in *A. nidulans* were then transformed with the *psi* BGC. Product formation was initially investigated in batch cultures for 48 h, comparing the strain expressing the *psi* cluster in a wild type (tJF03) (Hoefgen et al., 2018) versus the Δ *aroH* single mutants as background, which revealed a higher production of psilocybin (Figure 5). This effect was even more pronounced when both *aroH* genes were deleted, resulting in a 10 times higher production.

The best-producing strain, Δ *aroH1*/ Δ *aroH2*_psi, was chosen for further characterization and optimization of growth and product formation based on the online monitoring of the oxygen transfer rate (OTR) as well as carbon dioxide formation. *A. nidulans* Δ *aroH1*/ Δ *aroH2*_psi was compared to tJF03 and monitored for 192 h (Figure 6). Until 21 h, both strains grew exponentially to their maximal oxygen transfer rates of 23 mmol/L/h (Δ *aroH1*/ Δ *aroH2*_psi) and 24 mmol/L/h (tJF03) (Figure 6A). Although glucose was available at 21 h (Figure 6B), the OTR declined slowly, indicating a secondary substrate limitation (Anderlei & Büchs, 2001; Vrabl et al., 2019). Interestingly, the OTR and carbon dioxide transfer rate (CTR) of Δ *aroH1*/ Δ *aroH2*_psi peaked again shortly after induction, whereas a plateau was observed for tJF03. From 48 h on, the respiratory activity decreased for both strains, also caused by glucose exhaustion around 72 h (Δ *aroH1*/ Δ *aroH2*_psi) and until 96 h (tJF03). Due to the limitation of a second

substrate, biomass formation was limited at maximum cell dry weights (CDW) of 30 g/L (tJF03) and 28 g/L (Δ *aroH1*/ Δ *aroH2*_psi) after 96 h and 72 h. There was a considerable difference in pH between the two strains, with the Δ *aroH1*/ Δ *aroH2*_psi cultures becoming more acidic at pH 6.1 (48 h), compared to pH 6.5 for the tJF03 cultures. By HPLC analysis, 2 g/L succinic acid and 1.4 g/L fumaric acid were detected after 48 h, however, simulating these amounts in media were not leading to the same pH shift, leaving the causality for pH differences elusive. Generally, a growth deficit was not apparent, even though tryptophan catabolism is repressed in Δ *aroH1*/ Δ *aroH2*_psi.

Regarding psilocybin formation, a maximum of 267 mg/L was formed in Δ *aroH1*/ Δ *aroH2*_psi until 72 h (Figure 6C). This is fourfold higher and 1.7 times faster than the maximum of tJF03 with 66 mg/L at 120 h. Increased tryptophan, 4-hydroxytryptamine and norbaeocystin concentrations observed in the double mutant further prove the hypothesis that the cellular L-tryptophan pool is increased and preferentially routed towards psilocybin biosynthesis (Figure S3). Interestingly, no tryptamine was detected suggesting sufficient efficiency of PsiD. Compared to the initial expression test (Figure 5), the psilocybin concentration was increased 12-fold by increasing cultivation time and modifying cultivation conditions (induction time, temperature regime and pH buffering). Similar to the previous results, a considerable amount of the precursor baecocystin was formed (Figure 5). This is probably due to the inadequate amount of *psiM* present in the polycistronic *psi* cluster. A strategy to further optimize the product formation could be achieved by introduction of additional copies of the gene in the *psi* cluster similar to the reported *S. cerevisiae* strain by Milne et al. (2020). In contrast to the yeast strain, psilocin production comprised minor amounts for both strains in this study, showing a less diverse product spectrum and more specific psilocybin production. Finally, in this shake flask cultivation, 267 mg/L of psilocybin was produced in 72 h in *A. nidulans* Δ *aroH1*/ Δ *aroH2*_psi, resulting in a space–time–yield (STY) of 3.7 mg/L/h. Although this was only a batch process, the STY is even higher than the 2.9 mg/L/h (627 mg/L in 213.7 h) achieved by the engineered *S. cerevisiae* during the fed-batch bioprocess (Milne et al., 2020). A combination of both, the repression of catabolic pathways as well as the optimization of the biosynthetic pathway will probably lead to the highest psilocybin formation and will be matter of future investigations.

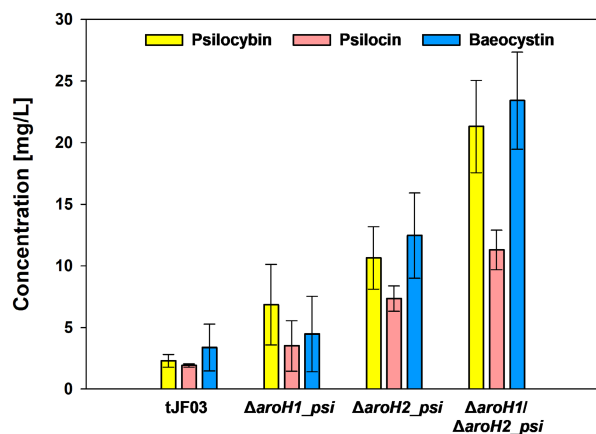


FIGURE 5 Psilocybin, psilocin and baecocystin production in *A. nidulans* mutant strains. Production of psilocybin, psilocin and baecocystin during shake flask cultivations of *A. nidulans* *aroH* single and double mutant strains expressing the *psi* cluster as a polycistron after 48 h (24 h post-induction). Data are presented as averages and error bars indicate the standard error.

CONCLUSION

Currently, the demand for psilocybin for clinical studies and pharmaceutical purposes is met by chemical synthesis. Engineered microorganisms represent a

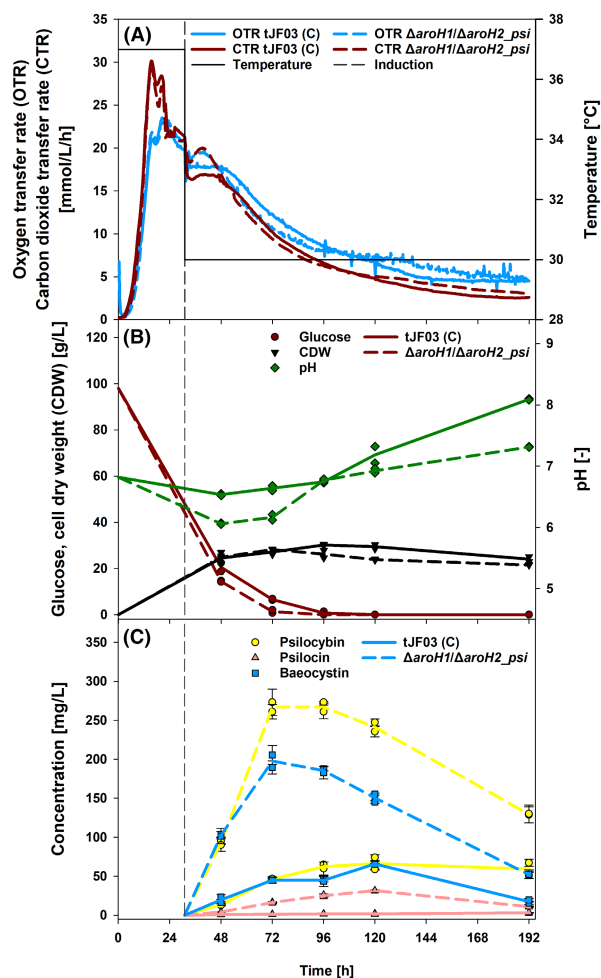


FIGURE 6 Process characterization and respiratory activity monitoring. (A) Online data of oxygen transfer rate (OTR) and carbon dioxide transfer rate (CTR) is shown for the *A. nidulans* double mutant $\Delta aroH1/\Delta aroH2$ and the control strain tJF03, both expressing the *psi* cluster as a polycistron. Induction was performed at 31 h upon decrease of metabolic activity observed by the decline in OTR signal. For improved enzyme production, the temperature was shifted to 30°C as indicated. (B) Offline data of glucose concentration, cell dry weight (CDW) and pH progression is shown over the cultivation time for both strains. (C) Production of psilocybin, psilocin and baecocystin over the time of cultivation for the wild type (tJF03) and double mutant backgrounds. Data are presented as averages from duplicate shake flask cultivations and triplicate product quantification with standard errors presented as error bars.

viable in vivo alternative to reconstitute metabolic pathways for biotechnological production. Fungal hosts offer proper posttranslational processing of enzymes as well as cofactors. Specific to pathways including P_{450} enzymes, such as for psilocybin, compatible cytochrome P_{450} reductases are intrinsically provided by the host cell. In this study, we successfully demonstrated the positive effect of tryptophan catabolism repression on biosynthesis of the tryptamine-derived prodrug psilocybin in *S. cerevisiae* and *A. nidulans*. Deletion of the aminotransferase genes *ARO8* and

ARO9 as well as the indoleamine 2,3-dioxygenase gene *BNA2* significantly increased psilocybin titres in *S. cerevisiae*. Genome mining of the *A. nidulans* genome revealed six genes coding for potential ARO-like aminotransferases, two of which were verified to complement the *S. cerevisiae* $\Delta aro8/\Delta aro9$ aminotransferase-deficient mutant. Simultaneous deletion of *aroH1* and *aroH2* in *A. nidulans* yielded a 10-fold increased psilocybin production. Characterization and initial optimization of the process with the engineered *A. nidulans* strain based on online respiratory activity measurement resulted in a titre of 267 mg/L psilocybin. These findings contribute to a better understanding of tryptophan catabolism in fungi and enable improved biosyntheses of tryptophan-derived alkaloids of pharmaceutical relevance in fungal hosts.

AUTHOR CONTRIBUTIONS

Slavica Janevska: Conceptualization; data curation; investigation; formal analysis; supervision; writing – original draft; funding acquisition. **Sophie Weiser:** Writing – review and editing; investigation; formal analysis; data curation; visualization. **Ying Huang:** Methodology; formal analysis; visualization. **Jun Lin:** Methodology; formal analysis; visualization. **Sandra Hoefgen:** Methodology; formal analysis; visualization. **Katarina Jojić:** Visualization; formal analysis. **Amelia E. Barber:** Methodology; formal analysis; visualization. **Tim Schäfer:** Formal analysis; visualization. **Janis Fricke:** Formal analysis; visualization. **Dirk Hoffmeister:** Supervision; funding acquisition; writing – review and editing. **Lars Regestein:** Formal analysis; supervision; funding acquisition; project administration. **Vito Valiante:** Writing – original draft; visualization; funding acquisition; supervision. **Johann E. Kufs:** Conceptualization; writing – review and editing; project administration; visualization; supervision.

ACKNOWLEDGEMENTS

We thank Daniela Hildebrandt for her excellent technical support. This work was supported by the Leibniz Research Cluster in the frame of the BMBF Strategic Process Biotechnology 2020+ (V.V.) and by a grant from the Free State of Thuringia and the European Social Fund (project HoWi, 2019FGR0079, L.R., S.W.). Work in S.J.'s laboratory is currently supported by a grant from the Free State of Thuringia and the European Social Fund Plus (project FusInfect, 2022FGR0007). Work in D.H.'s laboratory is funded by the Deutsche Forschungsgemeinschaft (DFG, German Research Foundation)—SFB 1127, Project-ID 239748522 and under Germany's Excellence Strategy—EXC 2051, Project-ID 390713860. S.W. and D.H. are authorized to handle controlled compounds according to the Narcotics Act of the Federal Republic of Germany.

CONFLICT OF INTEREST STATEMENT

The authors declare no competing interests.

DATA AVAILABILITY STATEMENT

The data that support the findings of this study are available from the corresponding author upon reasonable request.

ORCID

Slavica Janevska  <https://orcid.org/0000-0001-7361-495X>

Sophie Weiser  <https://orcid.org/0009-0004-6961-143X>

Sandra Hoefgen  <https://orcid.org/0000-0002-6806-7063>

Johann E. Kufs  <https://orcid.org/0000-0002-1177-2255>

REFERENCES

- Adams, A.M., Kaplan, N.A., Wei, Z., Brinton, J.D., Monnier, C.S., Enacopol, A.L. et al. (2019) In vivo production of psilocybin in *E. coli*. *Metabolic Engineering*, 56, 111–119.
- Anderlei, T. & Büchs, J. (2001) Device for sterile online measurement of the oxygen transfer rate in shaking flasks. *Biochemical Engineering Journal*, 7, 157–162.
- Blei, F., Baldeweg, F., Fricke, J. & Hoffmeister, D. (2018) Biocatalytic production of psilocybin and derivatives in tryptophan synthase-enhanced reactions. *Chemistry—a European Journal*, 24, 10028–10031.
- Bok, J.W., Hoffmeister, D., Maggio-Hall, L.A., Murillo, R., Glasner, J.D. & Keller, N.P. (2006) Genomic mining for aspergillus natural products. *Chemistry & Biology*, 13, 31–37.
- Bouhired, S., Weber, M., Kempf-Sontag, A., Keller, N.P. & Hoffmeister, D. (2007) Accurate prediction of the *Aspergillus nidulans* terrequinone gene cluster boundaries using the transcriptional regulator LaeA. *Fungal Genetics and Biology*, 44, 1134–1145.
- Caesar, L.K., Robey, M.T., Swyers, M., Islam, M.N., Ye, R., Vagadia, P.P. et al. (2020) Heterologous expression of the unusual terreezpine biosynthetic gene cluster reveals a promising approach for identifying new chemical scaffolds. *MBio*, 11, e01691-20.
- Camacho, C., Coulouris, G., Avagyan, V., Ma, N., Papadopoulos, J., Bealer, K. et al. (2009) BLAST+: architecture and applications. *BMC Bioinformatics*, 10, 421.
- Chen, L., Tang, J.W., Liu, Y.Y. & Matsuda, Y. (2022) Aspcandine: a pyrrolobenzazepine alkaloid synthesized by a fungal nonribosomal peptide synthetase-polyketide synthase hybrid. *Organic Letters*, 24, 4816–4819.
- Choera, T., Zelante, T., Romani, L. & Keller, N.P. (2017) A multifaceted role of tryptophan metabolism and indoleamine 2,3-dioxygenase activity in *Aspergillus fumigatus*-host interactions. *Frontiers in Immunology*, 8, 1996.
- Dindo, M., Costanzi, E., Pieroni, M., Costantini, C., Annunziato, G., Bruno, A. et al. (2018) Biochemical characterization of *Aspergillus fumigatus* AroH, a putative aromatic amino acid aminotransferase. *Frontiers in Molecular Biosciences*, 5, 104.
- Edgar, R.C. (2004) MUSCLE: multiple sequence alignment with high accuracy and high throughput. *Nucleic Acids Research*, 32, 1792–1797.
- Flower, J.E., Gibbons, W.J., Jr., Adams, A.M., Wang, X., Broude, C.N. & Jones, J.A. (2023) Biosynthesis of psilocybin and its nonnatural derivatives by a promiscuous psilocybin synthesis pathway in *Escherichia coli*. *Biotechnology and Bioengineering*, 120, 2214–2229.
- Fricke, J., Blei, F. & Hoffmeister, D. (2017) Enzymatic synthesis of psilocybin. *Angewandte Chemie, International Edition*, 56, 12352–12355.
- Fricke, J., Lenz, C., Wick, J., Blei, F. & Hoffmeister, D. (2019) Production options for psilocybin: making of the magic. *Chemistry—a European Journal*, 25, 897–903.
- Furter, R., Paravicini, G., Aebi, M., Braus, G., Prantl, F., Niederberger, P. et al. (1986) The TRP4 gene of *Saccharomyces cerevisiae*: isolation and structural analysis. *Nucleic Acids Research*, 14, 6357–6373.
- Goodwin, G.M., Aaronson, S.T., Alvarez, O., Arden, P.C., Baker, A., Bennett, J.C. et al. (2022) Single-dose psilocybin for a treatment-resistant episode of major depression. *New England Journal of Medicine*, 387, 1637–1648.
- Hoefgen, S., Lin, J., Fricke, J., Stroe, M.C., Mattern, D.J., Kufs, J.E. et al. (2018) Facile assembly and fluorescence-based screening method for heterologous expression of biosynthetic pathways in fungi. *Metabolic Engineering*, 48, 44–51.
- Hofmann, A., Heim, R., Brack, A., Kobel, H., Frey, A., Ott, H. et al. (1959) Psilocybin und Psilocin, zwei psychotrope Wirkstoffe aus mexikanischen Rauschpilzen. *Helvetica Chimica Acta*, 42, 1557–1572.
- Iraqui, I., Vissers, S., Cartiaux, M. & Urrestarazu, A. (1998) Characterisation of *Saccharomyces cerevisiae* ARO8 and ARO9 genes encoding aromatic aminotransferases I and II reveals a new aminotransferase subfamily. *Molecular & General Genetics*, 257, 238–248.
- Janevska, S., Ferling, I., Jojić, K., Rautschek, J., Hoefgen, S., Proctor, R.H. et al. (2020) Self-protection against the sphingolipid biosynthesis inhibitor fumonisin B₁ is conferred by a *FUM* cluster-encoded ceramide synthase. *MBio*, 11, e00455-20. Available from: <https://doi.org/10.1128/mbio.00455-00420>
- Jensen, M.E., Stenbæk, D.S., Juul, T.S., Fisher, P.M., Ekstrøm, C.T., Knudsen, G.M. et al. (2022) Psilocybin-assisted therapy for reducing alcohol intake in patients with alcohol use disorder: protocol for a randomised, double-blinded, placebo-controlled 12-week clinical trial (the QUANTUM trip trial). *BMJ Open*, 12, e066019.
- Jones, D.T., Taylor, W.R. & Thornton, J.M. (1992) The rapid generation of mutation data matrices from protein sequences. *Bioinformatics*, 8, 275–282.
- Kalyaanamoorthy, S., Minh, B.Q., Wong, T.K.F., von Haeseler, A. & Jermiin, L.S. (2017) ModelFinder: fast model selection for accurate phylogenetic estimates. *Nature Methods*, 14, 587–589.
- Kim, H.T., Na, B.K., Chung, J., Kim, S., Kwon, S.K., Cha, H. et al. (2018) Structural basis for inhibitor-induced hydrogen peroxide production by kynurenine 3-monooxygenase. *Cell Chemical Biology*, 25, 426–438.e424.
- Kispal, G., Csere, P., Prohl, C. & Lill, R. (1999) The mitochondrial proteins Atm1p and Nfs1p are essential for biogenesis of cytosolic Fe/S proteins. *The EMBO Journal*, 18, 3981–3989.
- Krappmann, S., Jung, N., Medic, B., Busch, S., Prade, R.A. & Braus, G.H. (2006) The *Aspergillus nidulans* F-box protein GrrA links SCF activity to meiosis. *Molecular Microbiology*, 61, 76–88.
- Lee, J.W., Na, D., Park, J.M., Lee, J., Choi, S. & Lee, S.Y. (2012) Systems metabolic engineering of microorganisms for natural and non-natural chemicals. *Nature Chemical Biology*, 8, 536–546.
- Li, H., Gilchrist, C.L.M., Phan, C.S., Lacey, H.J., Vuong, D., Moggach, S.A. et al. (2020) Biosynthesis of a new benzazepine alkaloid nanangelenin from *Aspergillus nanangensis* involves an unusual L-kynurenine-incorporating NRPS catalyzing regioselective lactamization. *Journal of the American Chemical Society*, 142, 7145–7152.
- Liu, X., Wang, L., Choera, T., Fang, X., Wang, G., Chen, W. et al. (2023) Paralogous FglDO genes with differential roles in

- tryptophan catabolism, fungal development and virulence in *Fusarium graminearum*. *Microbiological Research*, 272, 127382.
- Milne, N., Thomsen, P., Mølgaard Knudsen, N., Rubaszka, P., Kristensen, M. & Borodina, I. (2020) Metabolic engineering of *Saccharomyces cerevisiae* for the de novo production of psilocybin and related tryptamine derivatives. *Metabolic Engineering*, 60, 25–36.
- Minh, B.Q., Schmidt, H.A., Chernomor, O., Schrepf, D., Woodhams, M.D., von Haeseler, A. et al. (2020) IQ-TREE 2: new models and efficient methods for phylogenetic inference in the genomic era. *Molecular Biology and Evolution*, 37, 1530–1534.
- Ohashi, K., Chaleckis, R., Takaine, M., Wheelock, C.E. & Yoshida, S. (2017) Kynurenine aminotransferase activity of Aro8/Aro9 engage tryptophan degradation by producing kynurenic acid in *Saccharomyces cerevisiae*. *Scientific Reports*, 7, 12180.
- Panozzo, C., Nawara, M., Suski, C., Kucharczyka, R., Skoneczny, M., Bécam, A.M. et al. (2002) Aerobic and anaerobic NAD⁺ metabolism in *Saccharomyces cerevisiae*. *FEBS Letters*, 517, 97–102.
- Peck, S.K., Shao, S., Gruen, T., Yang, K., Babakanian, A., Trim, J. et al. (2023) Psilocybin therapy for females with anorexia nervosa: a phase 1, open-label feasibility study. *Nature Medicine*, 29, 1947–1953.
- Pedras, M.S., Yu, Y., Liu, J. & Tandron-Moya, Y.A. (2005) Metabolites produced by the phytopathogenic fungus *Rhizoctonia solani*: isolation, chemical structure determination, syntheses and bioactivity. *Zeitschrift für Naturforschung Section C*, 60, 717–722.
- Qian, Z.G., Xia, X.X. & Lee, S.Y. (2011) Metabolic engineering of *Escherichia coli* for the production of cadaverine: a five carbon diamine. *Biotechnology and Bioengineering*, 108, 93–103.
- Reimer, C., Kufs, J.E., Rautschek, J., Regestein, L., Valiante, V. & Hillmann, F. (2022) Engineering the amoeba *Dictyostelium discoideum* for biosynthesis of a cannabinoid precursor and other polyketides. *Nature Biotechnology*, 40, 751–758.
- Sayers, E.W., Beck, J., Bolton, E.E., Bourexis, D., Brister, J.R., Canese, K. et al. (2021) Database resources of the national center for biotechnology information. *Nucleic Acids Research*, 49, D10–D17.
- Schneider, P., Weber, M., Rosenberger, K. & Hoffmeister, D. (2007) A one-pot chemoenzymatic synthesis for the universal precursor of antidiabetes and antiviral bis-indolylquinones. *Chemistry & Biology*, 14, 635–644.
- Seibold, P.S., Dörner, S., Fricke, J., Schäfer, T., Beemelmans, C. & Hoffmeister, D. (2024) Genetic regulation of L-tryptophan metabolism in *Psilocybe mexicana* supports psilocybin biosynthesis. *Fungal Biology and Biotechnology*, 11, 4.
- Spizzichino, S., Pampalone, G., Dindo, M., Bruno, A., Romani, L., Cutruzzolà, F. et al. (2022) Crystal structure of *Aspergillus fumigatus* AroH, an aromatic amino acid aminotransferase. *Proteins*, 90, 435–442.
- Vrabl, P., Schinagl, C.W., Artmann, D.J., Heiss, B. & Burgstaller, W. (2019) Fungal growth in batch culture—what we could benefit if we start looking closer. *Frontiers in Microbiology*, 10, 2391.
- Wang, J., Chitsaz, F., Derbyshire, M.K., Gonzales, N.R., Gwadz, M., Lu, S. et al. (2023) The conserved domain database in 2023. *Nucleic Acids Research*, 51, D384–D388.
- Wogulis, M., Chew, E.R., Donohoue, P.D. & Wilson, D.K. (2008) Identification of formyl kynurenine formamidase and kynurenine aminotransferase from *Saccharomyces cerevisiae* using crystallographic, bioinformatic and biochemical evidence. *Biochemistry*, 47, 1608–1621.
- Yu, G., Smith, D.K., Zhu, H., Guan, Y. & Lam, T.T.-Y. (2017) GGTREE: an R package for visualization and annotation of phylogenetic trees with their covariates and other associated data. *Methods in Ecology and Evolution*, 8, 28–36.
- Yuasa, H.J. & Ball, H.J. (2011) Molecular evolution and characterization of fungal indoleamine 2,3-dioxygenases. *Journal of Molecular Evolution*, 72, 160–168.
- Zelante, T., Choera, T., Beauvais, A., Fallarino, F., Paolicelli, G., Pieraccini, G. et al. (2021) *Aspergillus fumigatus* tryptophan metabolic route differently affects host immunity. *Cell Reports*, 34, 108673.

SUPPORTING INFORMATION

Additional supporting information can be found online in the Supporting Information section at the end of this article.

How to cite this article: Janevska, S., Weiser, S., Huang, Y., Lin, J., Hoefgen, S., Jojić, K. et al. (2024) Optimized psilocybin production in tryptophan catabolism-repressed fungi. *Microbial Biotechnology*, 17, e70039. Available from: <https://doi.org/10.1111/1751-7915.70039>